THE JOURNAL OF PHYSICAL CHEMISTRY A

Article

pubs.acs.org/JPCA

Near-Infrared Surface-Enhanced Raman Spectroscopy (NIR-SERS) for the Identification of Eosin Y: Theoretical Calculations and Evaluation of Two Different Nanoplasmonic Substrates

Nathan G. Greeneltch,[†] Amber S. Davis,[†] Nicholas A. Valley,[†] Francesca Casadio,[‡] George C. Schatz,[†] Richard P. Van Duyne,[†] and Nilam C. Shah[†]

[†]Department of Chemistry, Northwestern University, Evanston, Illinois 60201, United States

[‡]The Art Institute of Chicago, 111 S. Michigan Ave., Chicago, Illinois 60603, United States

ABSTRACT: This work demonstrates the development of near-infrared surface-enhanced Raman spectroscopy (NIR-SERS) for the identification of eosin Y, an important historical dye. NIR-SERS benefits from the absence of some common sources of SERS signal loss including photobleaching and plasmonic heating, as well as an advantageous reduction in fluorescence, which is beneficial for art applications. This work also represents the first rigorous comparison of the enhancement factors and the relative merits of two plasmonic substrates utilized in art applications; namely, citrate-reduced silver colloids and metal film over nanosphere (FON) substrates. Experimental spectra are correlated in detail with theoretical absorption and Raman spectra calculated using time-dependent density functional theory (TDDFT) in order to elucidate molecular structural information and avoid relying on pigment spectral libraries for dye identification.

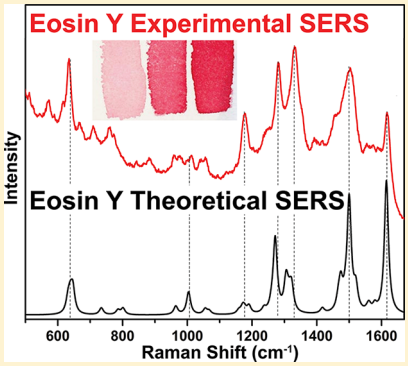

INTRODUCTION

Eosin Y is a fluorone dye belonging to the xanthene group ($C_{20}H_6O_5Br_4Na_2$; C.I. 45380; acid red 87), first synthesized by Caro in 1871 by brominating fluorescein in ethanolic or aqueous solution and subsequently converting it into the disodium salt.[1] Eosin was extensively used by 19th century artists, most notably by Vincent Van Gogh (1853−1890) specifically after 1888,[2] as well as in the textile dying industry and for printing inks.[3] In addition to its importance as an artists' pigment, eosin Y is used as a biological stain[4] and in photovoltaics.[5]

The bright fuchsia pigment, sold by color makers as a lake pigment (after precipitation with alum) with the name Geranium lake, is notoriously prone to rapid fading. As a result, there are several paintings by Van Gogh where only minute remnants of color are visible today on an otherwise completely discolored whitish-yellowish paint.[6] Thus, the motivation for this work is to develop ultrasensitive methods of identification for eosin Y when few pigment particles coated heavily with an organic medium (typically a lipidic binder, as these colorants were often used for transparent glazes) remain. The FT-Raman spectrum of bulk powder eosin Y pigment is obtainable; however, it requires low laser powers and long acquisition times to achieve acceptable signal/noise levels. It is not possible to record an FT-Raman spectrum when only a grain or two of pigment is available, as is often the case with high-valued artwork. This problem is overcome by utilizing surface-enhanced Raman spectroscopy (SERS), which can identify extremely small amounts of material (i.e., ∼femtograms),[7] as is typically accessible in a museum setting.

SERS, discovered in 1977,[8] is characterized by the enhancement in Raman scattered intensity observed when molecules are brought into close (0−2 nm) proximity of nanoscale roughened noble metal surfaces.[9] Intensified local electromagnetic fields resulting from localized surface plasmon resonance (LSPR) of the nanoscale structures have been shown[10] to enhance the observed Raman signal by a factor of 10^6−10^8. The plasmonic properties of metallic nanostructures are crucially dependent on structural geometry,[11] and increasing the aspect ratio of immobilized SERS-active nanostructures results in a red-shift of the LSPR λ_{max}.[12] At the ensemble average level, the maximum SERS signal enhancement (due to electromagnetic effects[13]) is achieved when the LSPR λ_{max} of the substrate lies between the wavelength of the laser and the wavelength of the Stokes-shifted Raman photon.[14] Therefore, tunability of the SERS-active substrate is highly desirable because maximum enhancement can be obtained for different excitation wavelengths.

The choice of excitation wavelength in a study is a complex one. Exciting near a molecular absorption resonance (for example, eosin Y is located at 521 nm) will increase returned signal and is known as surface-enhanced resonance Raman spectroscopy (SERRS).[15] SERRS was recently used in single-molecule Raman measurements of rhodamine 6G[16] and crystal violet.[17] For many art applications, the use of lasers with excitation wavelengths shorter than 785 nm will also cause fluorescence of the binding media and of some organic pigments, which results in the appearance of large, broad background features. This is especially true when the colorant of interest is used for paints or glazes that are

Received: August 14, 2012
Revised: October 24, 2012
Published: October 26, 2012

   dx.doi.org/10.1021/jp3081035 | J. Phys. Chem. A 2012, 116, 11863−11869

medium-rich, possibly highly oxidized, and therefore highly fluorescent. In addition, visible laser irradiation produces photobleaching[18] and plasmonic heating,[19] which also reduce the SERS signal. The latter effect scales directly with the source intensity and molecular absorption cross-section.[20] Thus, the use of near-infrared wavelengths and low power densities is highly desirable.

SERS has been demonstrated as an effective and extremely sensitive tool for the identification of organic colorants used in paints, glazes, and textiles on a variety of works of art from different cultures and epochs.[21] With few exceptions, these studies focused on organic colorants of natural origin[22] using a limited range of plasmonic substrates, sample pretreatment routines,[23] and excitation wavelengths typically in the visible range. In this article, we extend the utility of SERS for characterization of important historical dyes by detecting eosin Y at near-infrared wavelengths (785 and 1064 nm) using two substrates and correlating experiments with TDDFT calculations. In parallel SERS measurements, the commonly used mobile Lee−Meisel colloid substrate[24] is compared and contrasted with a high-performance immobilized metal film over nanosphere (FON) substrate. While these systems have been separately used for art research,[25] this work presents, for the first time, a rigorous comparison of their relative merits and Raman enhancements. The colloidal substrate does not require preanalysis extraction of the colorants of interest, which may be advantageous for use in art field studies. However, immobilized FON substrates, while requiring extraction, do possess a tunable plasmon resonance, which can be optimized for use anywhere in the visible and near-infrared spectral windows.

Additionally, this research presents the full TDDFT-derived Raman spectrum of eosin Y. These calculations allow for a deeper understanding of eosin Y's molecular Raman modes. This represents an important step in the development of an alternative approach to using empirically developed SERS spectral libraries for dye identification. While these libraries have been presented for natural colorants used in art applications,[26] given the thousands of colorants patented after 1856 (when William H. Perkin derived mauveine from coal tar), an alternative approach to acquiring reference samples and measuring the SER spectra of all historically important synthetic art dyes will prove valuable. In summary, this work demonstrates the feasibility of SERS analysis of eosin Y at near-infrared wavelengths. This approach benefits from removal of fluorescence and common sources of SERS signal loss, leading to higher SERS enhancement.

EXPERIMENTAL SECTION

Metal Film-Over-Nanosphere (FON) Substrate Fabrication. Glass coverslips (Fisherbrand, #1s) and polished Silicon wafers (MEMC Electronics) were used as supports for SERS substrates made as described in prior publications.[27] Silica (Bangs Laboratories) nanospheres were diluted to 5% by volume. The manufacturer's solvent was replaced twice with Millipore (Milli-Q, 18.2 MΩ cm^{-1}) ultrapure H_2O by conventional centrifugation/supernatant removal procedure, followed by sonication for a minimum of 1 h. Substrates were prepared by drop coating 7−10 μL of solvent followed by manual nanosphere assembly on the silicon support wafer. The solvent was then allowed to evaporate in ambient conditions, leaving a close-packed array of nanospheres. SiO_2 spheres with diameters of 390, 570, and 780 nm were used for SERS studies with excitation sources of 532, 785, and 1064 nm, respectively. Gold (150 nm thick) was then deposited at a rate of 3 Å s^{-1} under high vacuum (2.0×10^{-7} Torr) over the nanosphere-covered surface using physical vapor deposition (Kurt J. Lesker PVD 75). The substrates were held normal to the metal plume during deposition, while Au mass thickness and deposition rate were measured by a 6 MHz gold-plated quartz crystal microbalance purchased from Sigma Instruments (Fort Collins, CO).

Colloid Substrate Preparation. A silver colloidal paste for SERS analyses was prepared as described previously.[25a] Briefly, citrate-reduced silver colloids were synthesized using the standard Lee and Meisel procedure.[24] Silver nitrate (99+%) was purchased from Sigma-Aldrich (St. Louis, MO) and sodium citrate dihydrate from Mallinckrodt, Inc. (St. Louis, MO). After the colloidal solution cooled, it was centrifuged (at 3600 relative centrifugal force, 15 min per cycle), and the supernatant was replaced with more colloidal solution ten times to concentrate and aggregate the colloids further. The LSPR λ_{max} of the resultant paste was 492 nm.

Dye Solution and SERS Substrate Procedure. Eosin Y (99%, Sigma-Aldrich) was used without further purification. A solution of 10 mM eosin Y was prepared in 50% methanol/water (v/v) (HPLC grade methanol, EMD Chemicals Inc., Gibbstown, NJ), and the pH was adjusted to 8.0 with a 1 M aqueous sodium hydroxide solution (Mallinckrodt, Inc.). To conduct SERS analyses of eosin Y on colloids, 5 μL of dye solution and 5 μL of colloid paste were pipetted onto a glass microscope slide and mixed thoroughly then allowed to dry. The AuFONs were incubated in 1 mL of dye solution for 1 h, then rinsed with methanol and allowed to dry.

UV/Vis Absorbance and Reflectance Measurements. A Cary 5000 UV−vis-NIR spectrophotometer (Varian, Inc., Palo Alto, CA) was used to collect absorbance spectra of 5 μM eosin Y in 50% methanol/water (v/v) as a function of pH. The eosin Y solution's pH was adjusted with 1 M aqueous sodium hydroxide. Spectra were collected in glass cuvettes (Starna Cells, Inc., Atascadero, CA), and collection parameters were as follows: 0.1 s integration per data point, 0.2 nm data point intervals, λ = 400−600 nm.

The LSPR spectra of FONs were collected by using the Cary 5000 UV−vis-NIR spectrophotometer in diffuse reflectance mode. Collection parameters were as follows: 0.1 s integration per data point, 1 nm data point intervals, λ = 200−1300 nm.

SERS Measurements. An inverted microscope (Nikon Eclipse Ti-U) was used for all Raman measurements. A series of diode based lasers were used for single frequency experiments, including (1) Spectra Physics Excelsior 1064 nm, (2) Innovative Photonics Solutions stabilized 785 nm, and (3) Spectra Physics Excelsior 532 nm. The detection system for 785 and 532 nm studies was an imaging spectrograph (Acton SpectraPro 2300i) with a liquid nitrogen cooled back-thinned deep-depletion CCD detector (Roper, Model Spec 10:400BR, 1340 × 400 pixels). A second detection system was used for IR Raman studies, consisting of a spectrograph (Acton SpectraPro 2300i) configured for IR wavelengths along with a liquid nitrogen cooled InGaAs Array detector (Roper, Model OMA V 1024−1.7, 1024 pixels). The excitation sources were introduced through the back entrance of the microscope and then focused down to a 70 × 70 μm spot at the sample using an ELWD S Plan Fluor 20× microscope objective.

Theoretical Calculations. Electronic structure calculations were performed using the Amsterdam Density Functional (ADF) program package.[28] Full geometry optimization, frequency, and response calculations for the anion and dianion of eosin were completed using the Becke−Perdew (BP86) XC-potential and a triple-ζ polarized Slater type (TZP) basis set. Relativistic effects

for the bromine atoms were included by use of the zeroth order regular approximation (ZORA). Solvation was modeled using the conductor-like screening model (COSMO). Default values for water were applied. Nonequilibrium solvation was used for response calculations with a nonequilibrium dielectric constant of 1.78.

The lowest 100 dipole-allowed transitions were calculated to generate the optical absorption spectrum of each species. Polarizabilities were calculated using the AORESPONSE module. Polarizabilities on resonance were calculated using a global damping parameter of $\Gamma = 0.004$ au (0.1 eV); this is the same as was used in earlier works[29] and is thought to represent a reasonable estimate of the excited state dephasing lifetime. Raman scattering cross-sections are calculated by[30]

$$\frac{d\sigma}{d\Omega} = \frac{\pi^2}{\varepsilon_0^2}(\omega - \omega_p)^4 \times \frac{h}{8\pi^2 c\omega_p}[45\bar{\alpha}'_p{}^2 + 7\gamma\bar{\alpha}'_p{}^2] \times \frac{1}{45(1 - e^{(-hc\omega_p/k_B T)})} \quad (1)$$

where ω and ω_p are the frequencies of the incident radiation and the pth vibrational mode, respectively, and the scattering factor $45\bar{\alpha}'_p + 7\gamma'_p$ is composed of the isotropic ($\bar{\alpha}'_p$) and anisotropic (γ'_p) polarizability derivatives with respect to the pth vibrational mode.

RESULTS AND DISCUSSION

UV/Vis Spectroscopy. Since all of the protolytic species of eosin Y potentially can be adsorbed and detected on a SERS substrate, it is important to identify the particular eosin Y species present in solution at a given pH. Speciation of hydroxyxanthene dyes in solution was previously investigated,[31] with 7 different possible forms (Figure 1; cation is not shown) reported depending on the pH and solvent of the system. Eosin Y is known to exist in two neutral forms: the lactone and the quinoid.[32] The concentration of the lactone is 1.8 times the concentration of the quinoid in water, and this ratio increases to 6.4 in methanol. The anionic form of eosin Y is known to exist as predominantly the phenolate anion; the relative concentration of the carboxylate anion is very low in water and negligible in organic solvents.[33] The first and second pK_a, which correspond to the formation of the anion and then the dianion, are 3.16 and 5.4 in 50% methanol/water, respectively.[34] Theoretical absorbance calculations (TDDFT) and UV/vis spectroscopy experiments were conducted to unambiguously identify and confirm the protolytic species present in the chosen solvent system and pH range.

A spectrophotometric titration of eosin Y in a 50% methanol/water environment is shown in Figure 2 (top left). Absorption increased with pH until the pH value of 5.5 was reached. At this point, a gradual blue-shift (from 527 to 521 nm) occurred, while the absorption continued to rise until pH 7.0. The absorption spectra did not change above pH 7.0 and therefore are not shown in Figure 2. The first and second pK_a values of eosin Y were used in conjunction with the Henderson–Hasselbalch equation to calculate estimated relative concentrations of the phenolate anion and dianion (Figure 1) at each sampled pH point. TDDFT absorbance spectra were then calculated for each species and combined, weighted by their calculated relative ratios as a function of pH (Figure 2, bottom left). Similar rise and blue-shift behavior was calculated as the dianionic species of eosin Y increased in concentration. The electronic transition of the dianion centered at 507 nm was determined to consist almost

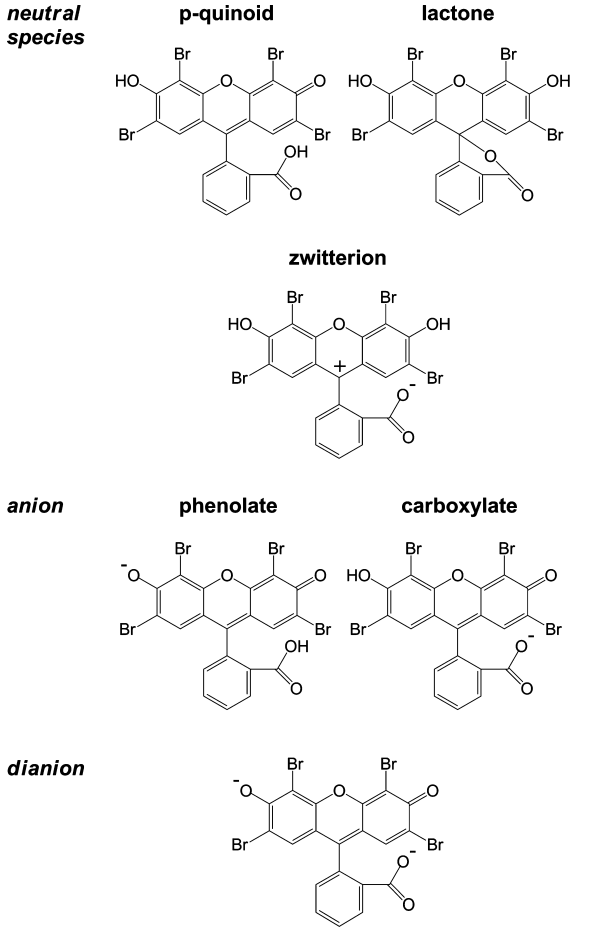

Figure 1. Chemical structures of eosin Y's protolytic species (cation not shown). The first (3.16) and second (5.4) pK_a values employed in the Henderson–Hasselbalch speciation analysis correspond to the formation of the anionic and the dianionic form, respectively.[34]

completely (94%) of highest occupied molecular orbital (HOMO) → lowest unoccupied molecular orbital (LUMO) character. The eosin Y dianion HOMO and LUMO molecular orbital diagrams are shown on the right side of Figure 2. A majority of the HOMO and LUMO is centered on the xanthene-like chromophore portion of the molecule. This fact is also consistent with eosin Y's high fluorescence quantum yield of 0.68.[35]

Together, the absorption spectroscopy experiment and the theoretically calculated absorbance titration demonstrate that, above pH 7 in 50% methanol/water, eosin Y is present exclusively in its dianionic form. SERS measurements were conducted at pH 8.0 because the dianionic form of eosin Y is used to manufacture the geranium lake pigment, and therefore, this form is most relevant to dye molecule sensing in art objects.

Theoretical Analysis of Eosin Y Raman Modes. Vibrational frequencies and Raman intensities of the dianionic form of eosin Y were calculated and compared to the experimental measurements (Figure 3). While the relative Raman intensities were in excellent agreement with experimental spectra, the calculated vibrational energies composing the most intense peaks were ~30 cm^{-1} lower than their experimental counterparts. We attribute this discrepancy to the lack of diffuse functions on the bromine atoms or to inaccuracy in the density functional being used. Upon further investigation, it was found that modes

dx.doi.org/10.1021/jp3081035 | J. Phys. Chem. A 2012, 116, 11863–11869

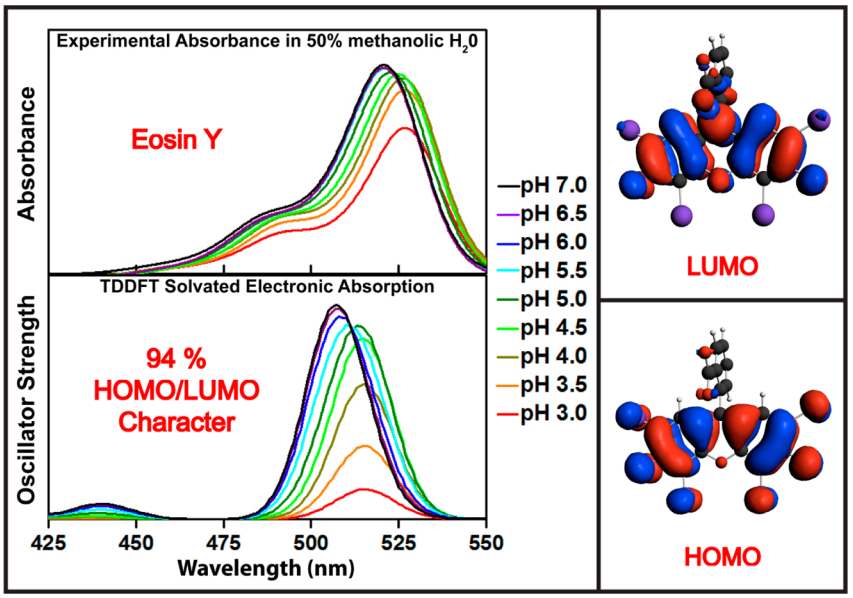

Figure 2. Experimental measurements (top, left) and theoretical calculations (bottom, left) of solvated eosin Y's visible absorption spectra. Plots are presented in arbitrary units. The HOMO and LUMO orbitals of eosin Y are shown on the right side (top and bottom) of the figure. TDDFT was used for all theoretical calculations.

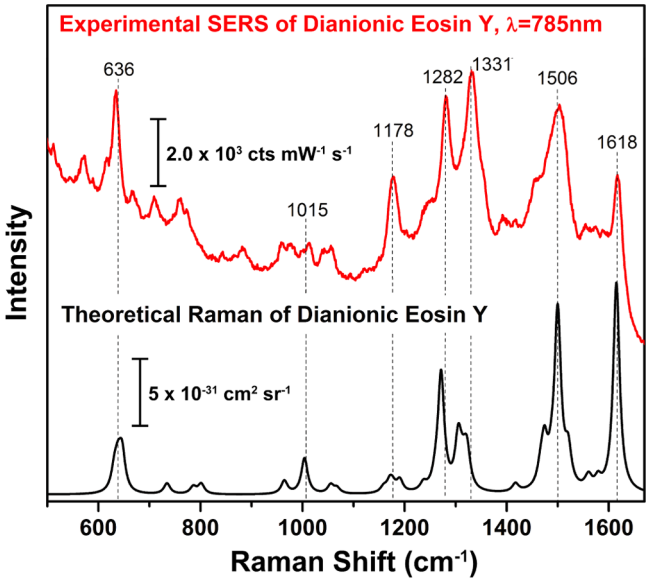

Figure 3. Comparison of eosin Y experimental SERS and theoretical Raman spectra. Experimental data was recorded with 785 nm excitation. Acquisition time and laser power were 10 s and 62.6 μW, respectively. A gold FON was used with 150 nm metal film on 600 nm silica nanospheres. The theoretical spectrum was calculated using TDDFT with the BP86 functional.

concentrated on the benzoate-like portion of the molecule were in close agreement in energies with the theoretical spectra of free benzoate. As a temporary solution, 30 cm^{-1} were added to the vibrational energies of the modes with substantial character on the xanthene-like ring portion of the molecule. These corrected energies are presented in Table 1 along with the calculated relative Raman intensity. Descriptions for each mode are also provided, and experimental peaks are matched with a theoretical mode or group of modes. As expected, the majority of the Raman intensity arises from the xanthene-like chromophore portion of the molecule.

SERS Analysis of Eosin Y on FON Substrates. A series of SERS measurements were carried out on AuFON substrates optimized for 532 nm (LSPR λ_{max} = 612), 785 nm (LSPR λ_{max} = 823), and 1064 nm (LSPR λ_{max} =1096) excitation wavelengths. The results are shown in Figure 4 together with average SERS enhancement factors (EF) for each substrate. The EFs presented are a lower bound estimate of the electromagnetic SERS enhancement imparted to surface-bound species. The EF is a fundamental property of the enhancing substrate and is given by the equation:

$$\mathrm{EF} = \frac{I_{\mathrm{SERS}}/N_{\mathrm{SERS}}}{I_{\mathrm{NRS}}/N_{\mathrm{NRS}}} \quad (2)$$

where I is the measured intensity and N is the number of molecules illuminated in the SERS measurement and solution-based normal Raman (NRS) measurement. The 640 cm^{-1} xanthene out-of-plane ring deformation mode (see Table 1) was chosen for EF analysis due to its vibrational motion's high character normal to the surface, maximizing its coupling to the enhanced electric field. The radial coverage of molecules (N_{SERS}) was calculated using the maximum geometrically allowed packing density given the theoretically determined eosin Y footprint (from the optimized geometry) of 144 $Å^2$.

Spectroscopic measurements with the 1064 nm laser produced 20.8 times the SERS EF of those performed with the 785 nm laser. In contrast, the normalized Raman intensity diminished with increased wavelength. The SERS signal decreased by an order of magnitude between the 532 and 785 nm source measurements and by more than 2 orders of magnitude between the 785 and 1064 nm source measurements. As experiments were moved to the red, observed signal loss was due to the Raman scattering efficiency's fourth-power dependence on the excitation frequency.[36] The corresponding rise in EF is explained by the higher electric field enhancements imparted to SERS substrates optimized in this region,[12] as well as the reduction of fluorescent photobleaching and plasmonic heating.

dx.doi.org/10.1021/jp3081035 | J. Phys. Chem. A 2012, 116, 11863−11869

Table 1. Static TDDFT Theoretical Eosin Y Raman Mode Descriptions with Experimental Peak Locations for 785 and 532 nm Excitation Spectra Included As Denoted in Far-Right Column; the Theoretical Spectrum Was Calculated Using TDDFT with the BP86 Functional; Asterisks Denote Unshifted Vibrational Energies

shifted calculated mode (cm^{-1})	relative intensity	description	785 nm (532 nm) experimental peak (cm^{-1})
350	72	xanthene ring-Br stretches	
407.4	287	xanthene breathing + Bz ring/ CO_2 stretch	
631.6	179	xanthene breathing + Bz breathing	636 (641)
638.6	215	xanthene out of plane ring deformation	
646.4	327	xanthene ring stretches + Bz ring stretch	
734.5	113	xanthene out of plane ring deformation	709 (711)
785.9	82	xanthene ring stretches	782 (775)
*801.5	119	Bz ring stretch and CO_2 bend	
964.3	199	xanthene and Bz ring stretches	965 (959)
1003.8	575	xanthene ring breathing + C−Br stretches	1015 (1016)
1055.3	149	xanthene ring C−C stretches	1040
*1067.6	94	Bz ring stretch and sym CO_2 stretch	1059
1158.9	106	xanthene and Bz ring stretches and sym CO_2 stretch	1178(1175)
1171.2	217	xanthene ring stretches and Bz ring breathing	
1176.6	128	xanthene ring C−O/C−C stretches	
1190.5	249	xanthene ring C−C stretches	
1236.8	161	xanthene ring C−O/C−C stretches	1236
1260.4	203	xanthene and Bz ring C−C stretches	1282 (1279)
1271.5	2639	xanthene and Bz ring C−C stretches	
1305	1126	xanthene and Bz ring C−C stretches	1331 (1313)
*1310.9	253	Bz ring stretch and sym CO_2 stretch	
*1317.1	333	Bz ring stretch and sym CO_2 stretch	
1322.5	817	xanthene and Bz ring C−C stretches	
1417.3	213	xanthene ring C−C stretches	(1415)
1466.6	444	xanthene ring C−C stretches	(1472)
1474	1180	xanthene (perp) and Bz ring C−C stretches	
1488	413	xanthene (perp) and Bz ring C−C stretches	1506(1504)
1499.8	4816	xanthene and Bz ring C−C stretches	
*1504.1	371	Bz ring stretch and assym CO_2 stretch	
1520.6	1044	xanthene sym carbonyl C−O stretches	
*1555.9	73	Bz ring C−C stretches and assym CO_2 stretch	
1561	351	xanthene ring stretches + sym carbonyl C−O stretches	
*1579	323	Bz ring stretch	1574(1571)
1615	6785	xanthene ring C−C stretches	1618(1622)

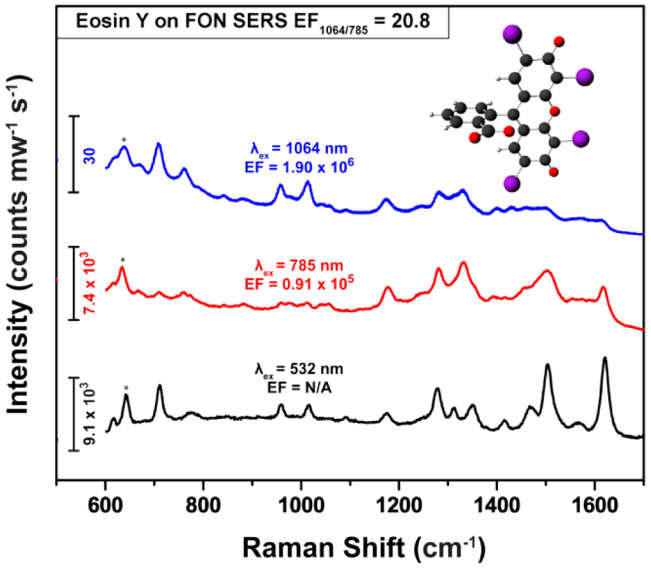

Figure 4. SERS spectra of eosin Y on metal FON substrates. Measurements were carried out on AuFON substrates optimized for 532 nm (LSPR λ_{max} = 612 nm), 785 nm (LSPR λ_{max} = 823 nm), and 1064 nm (LSPR λ_{max} = 1096 nm) excitation wavelengths. Enhancement factors (EF) were calculated as explained in the text using the 636 cm^{-1} peak, which is denoted with a star. The powers (P) and acquisition times (t) used to record spectra were as follows: P_{532} = 20.7 μW, P_{785} = 62.6 μW, P_{1064} = 21.5 mW and t_{532} = 15 s, t_{785} = 10 s, t_{1064} = 5 s.

The significantly higher SERS signals with 532 nm excitation are due to a coupling of eosin Y's molecular resonance with the excitation frequency leading to the SERRS phenomenon. Since this added enhancement was a consequence of the molecule−source interaction and not the substrate−source interaction, a FON substrate enhancement factor could not be accurately reported from this measurement. In addition, solution Raman was not successfully recorded at λ_{exc}= 532 nm due to molecular fluorescence overwhelming the resonance Raman signal. A preferential enhancement of the chromophore centered modes of the probe molecule was observed as is expected with SERRS.

SERS Analysis of Eosin Y on Colloid Substrates. SERS analysis was also performed on silver colloid substrates. The results of the study are presented in Figure 5. The colloidal assembly was illuminated with a penetration depth that could not be readily measured. The reported EF values assume only two-dimensional excitation (similar to FON substrates) and are therefore an overestimate of the substrate's EF. Comparison of the estimated EFs from the near-IR and infrared measurements show a much smaller increase in EF (2.65) compared to the FON (20.8) as the experimental excitation wavelength is moved to the red. This is due to the inability to tune the plasmon resonance of colloidal substrates. Another consequence of this limitation is the much steeper drop-off in returned SERS signal in the infrared measurements with colloids compared to that of the tunable FON substrate.

The complicated geometry of colloidal substrates impacts the analysis in multiple ways. As stated above, the probe penetration depth is unclear. In addition, the disordered assembly of the colloids and subsequent trapping of codeposited molecules also shields some surface sites from adsorption and oversaturates others. The unbound surface sites and occasional

dx.doi.org/10.1021/jp3081035 | J. Phys. Chem. A 2012, 116, 11863−11869

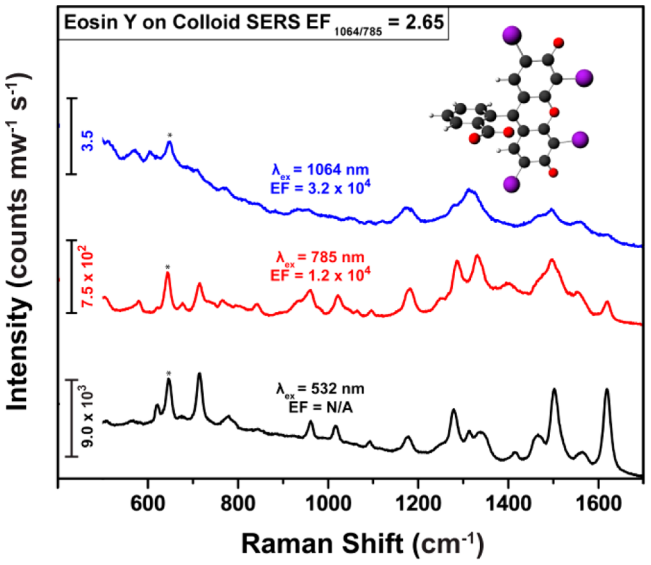

Figure 5. SERS spectra of eosin Y on colloid substrates (LSPR λ_{max} = 492 nm). Measurements were carried out at 532, 785, and 1064 nm excitation wavelengths. Enhancement factors (EF) were calculated as explained in the text using the 636 cm^{-1} peak, which is denoted with a star. The powers (P) and acquisition times (t) used to record spectra were as follows: P_{532} = 31.4 μW, P_{785} = 296 μW, P_{1064} = 182 mW and t_{532} = 10 s, t_{785} = 30 s, t_{1064} = 10 s.

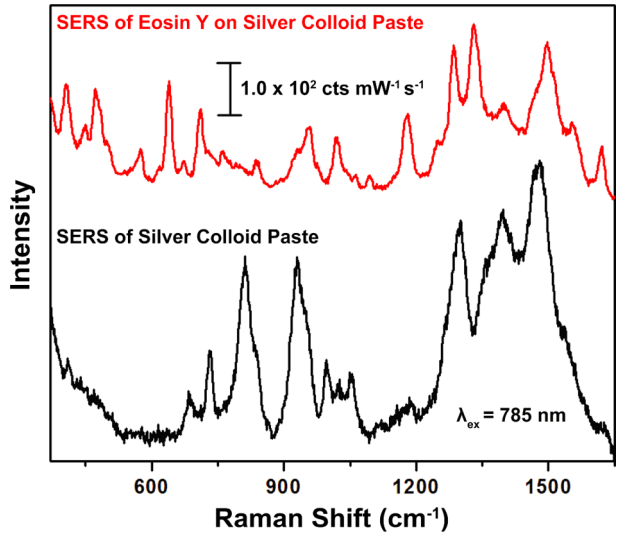

Figure 6. SERS spectra of eosin Y on colloid substrates (top) and bare colloid paste background (bottom). Measurements were carried out with 296 μW of 785 nm excitation wavelength. Acquisition time was 30 s.

fluorescent areas from local unbound molecules results in high background signal (Figure 6) and high spot-to-spot variation across the substrate. These phenomena are not observed using FON substrates. As a result, FON substrates return more highly reproducible spectra and display higher EFs than colloidal substrates; a fact exhibited by the largest enhancement factors reported in Figures 4 and 5 ($EF_{FON} = 1.90 \times 10^6$ and $EF_{colloid} = 3.2 \times 10^4$ with λ_{ex} = 1064 nm).

CONCLUSIONS

Shifting the SERS excitation to longer wavelengths can be advantageous for art applications, where binders, varnishes, and the colorant itself can contribute interfering fluorescence if excited at visible or UV wavelengths. This work demonstrates the successful identification of eosin Y using visible and deep NIR-SERS, coupled with complete band assignment using TDDFT theory. In practical cultural heritage applications, NIR-SERS measurements are required when sample damage is likely or fluorescence impurities contaminate the signal. Furthermore, this study demonstrates that FONs are the ideal substrate for pigment identification compared to Lee–Meisel colloids if particle mobility is not required. FONs can be optimized to give maximum EFs for the desired excitation wavelength, quench fluorescence, and have higher spot-to-spot signal reproducibility. This work also demonstrates that, although colloids cannot be optimized for a particular wavelength, it is possible to detect dyes with colloids at NIR wavelengths. In the future, we will use NIR-SERS to study the photodegradation mechanism of eosin Y and identify degradation species in works of art.

AUTHOR INFORMATION

Notes

The authors declare no competing financial interest.

ACKNOWLEDGMENTS

Conservation science research at the Art Institute of Chicago and Northwestern University is made possible by generous grants from the Andrew W. Mellon Foundation and the National Science Foundation (Grants: CHE-0414554, CHE-0911145, and DMR-1121262).

REFERENCES

(1) *Colour Index*; Society of Dyers and Colourists: Bradford, England, 1975; Vol. *6*, p 414.
(2) Rioux, J. P. *ICOM Committee for Conservation 12th Triennial Meeting*; James & James/Earthscan: London, England, 1999; pp 403–408.
(3) Hofenk de Graaff, J. H.; Karreman, M. F. S.; de Keijzer, M.; Roelofs, W. G. T. I. In *A Closer Look: Technical and Art-Historical Studies on Works by Van Gogh and Gauguin*; Peres, C., Hoyle, M., van Tilborgh, L., Eds.; Waanders Publishers: Zwolle, The Netherlands, 1991; Vol. *3*, pp 75–85.
(4) Lin, F.; Wise, G. E. I. In *The Protein Protocols Handbook* Walker, J. M., Ed.; Humana Press Inc: Totowa, NJ, 2009; pp 575–578.
(5) Mali, S. S.; Betty, C. A.; Bhosale, P. N.; Patil, P. S. *Electrochim. Acta* **2012**, *59*, 113–120.
(6) Burnstock, A.; Lanfear, I.; van den Berg, K. J.; Carlyle, L.; Clarke, M.; Hendriks, E.; Kirby, J. *ICOM Committee for Conservation 14th Triennial Meeting*, 12–16 September 2005; Verger, I., Ed. James & James/Earthscan: The Hague, The Netherlands, 2005; pp 459–466.
(7) Smith, W. E.; Rodger, C. I. In *Handbook of Vibrational Spectroscopy*; Chalmers, J. M., Griffiths, P. R., Eds.; John Wiley & Sons: Chichester, U.K., 2002; Vol. *1*, pp 775–784.
(8) Jeanmaire, D. L.; Van Duyne, R. P. *J. Electroanal. Chem. Interfacial Electrochem.* **1977**, *84*, 1–20.
(9) Moskovits, M. *Rev. Mod. Phys.* **1985**, *57*, 783–826.
(10) Biggs, K. B.; Camden, J. P.; Anker, J. N.; Van Duyne, R. P. *J. Phys. Chem. A* **2009**, *113*, 4581–4586.
(11) Kelly, K. L.; Coronado, E.; Zhao, L. L.; Schatz, G. C. *J. Phys. Chem. B* **2003**, *107*, 668–677.
(12) Arnold, M. D.; Blaber, M. G. *Opt. Express* **2009**, *17*, 3835–3847.
(13) Schatz, G. C.; Young, M. A.; Van Duyne, R. P. I. *Surface Enhanced Raman Scattering Physics and Applications*; Springer-Verlag: Berlin, Germany, 2006; Vol. *103*, pp 19–45.
(14) McFarland, A. D.; Young, M. A.; Dieringer, J. A.; Van Duyne, R. P. *J. Phys. Chem. B* **2005**, *109*, 11279–11285.

(15) (a) Zhao, J.; Sherry, L. J.; Schatz, G. C.; Van Duyne, R. P. *IEEE J. Sel. Top. Quantum Electron.* **2008**, *14*, 1418−1429. (b) Morton, S. M.; Jensen, L. *J. Am. Chem. Soc.* **2009**, *131*, 4090−4098.
(16) Dieringer, J. A.; Lettan, R. B., II; Scheidt, K. A.; Van Duyne, R. P. *J. Am. Chem. Soc.* **2007**, *129*, 16249−16256.
(17) Kleinman, S. L.; Ringe, E.; Valley, N.; Wustholz, K. L.; Phillips, E.; Scheidt, K. A.; Schatz, G. C.; Van Duyne, R. P. *J. Am. Chem. Soc.* **2011**, *133*, 4115−4122.
(18) (a) Sprague, B. L.; Pego, R. L.; Stavreva, D. A.; McNally, J. G. *Biophys. J.* **2004**, *86*, 3473−3495. (b) Lippincott-Schwartz, J.; Snapp, E.; Kenworthy, A. *Nat. Rev. Mol. Cell Biol.* **2001**, *2*, 444−456.
(19) (a) Govorov, A.; Zhang, W.; Skeini, T.; Richardson, H.; Lee, J.; Kotov, N. *Nanoscale Res. Lett.* **2006**, *1*, 84−90. (b) Govorov, A. O.; Richardson, H. H. *Nano Today* **2007**, *2*, 30−38.
(20) (a) Blaber, M. G.; Schatz, G. C. *Chem. Commun.* **2011**, *47*, 3769−3771. (b) Harris, N.; Ford, M. J.; Cortie, M. B. *J. Phys. Chem. B* **2006**, *110*, 10701−10707.
(21) Casadio, F.; Leona, M.; Lombardi, J. R.; Van Duyne, R. *Acc. Chem. Res.* **2011**, *44*, 238−238.
(22) Leona, M. *Proc. Natl. Acad. Sci. U.S.A.* **2009**, *106*, 14757−14762.
(23) Pozzi, F.; Lombardi, J. R.; Bruni, S.; Leona, M. *Anal. Chem.* **2012**, *84*, 3751−3757.
(24) Lee, P. C.; Meisel, D. *J. Phys. Chem.* **1982**, *86*, 3391−3395.
(25) (a) Brosseau, C. L.; Rayner, K. S.; Casadio, F.; Grzywacz, C. M.; Van Duyne, R. P. *Anal. Chem.* **2009**, *81*, 7443−7447. (b) Whitney, A. V.; Casadio, F.; Van Duyne, R. P. *Appl. Spectrosc.* **2007**, *61*, 994−1000.
(26) Bruni, S.; Guglielmi, V.; Pozzi, F. *J. Raman Spectrosc.* **2011**, *42*, 1267−1281.
(27) (a) Dick, L. A.; McFarland, A. D.; Haynes, C. L.; Van Duyne, R. P. *J. Phys. Chem. B* **2002**, *106*, 853−860. (b) Litorja, M.; Haynes, C. L.; Haes, A. J.; Jensen, T. R.; Van Duyne, R. P. *J. Phys. Chem. B* **2001**, *105*, 6907−6915.
(28) Baerends, E. J.; Ziegler, T.; Autschbach, J. A.; Bashford, D.; Berces, A.; Bickelhaupt, F. M.; Bo, C.; Boerrigter, P. M.; Cavallo, L.; Chong, D. P.; et al. *ADF2010*; SCM: Amsterdam, The Netherlands, 2010.
(29) (a) Zhao, L.; Jensen, L.; Schatz, G. C. *J. Am. Chem. Soc.* **2006**, *128*, 2911−2919. (b) Jensen, L.; Zhao, L. L.; Autschbach, J.; Schatz, G. C. *J. Chem. Phys.* **2005**, *123*, 174110/1−174110/11.
(30) Neugebauer, J.; Reiher, M.; Kind, C.; Hess, B. A. *J. Comput. Chem.* **2002**, *23*, 895−910.
(31) (a) Amat-Guerri, F.; Lopez-Gonzalez, M. M. C.; Sastre, R.; Martinez-Utrilla, R. *Dyes Pigm.* **1990**, *13*, 219−32. (b) McHedlov-Petrosyan, N. O.; Kukhtik, V. I.; Egorova, S. I. *Russ. J. Gen. Chem.* **2006**, *76*, 1607−1617. (c) Sjoback, R.; Nygren, J.; Kubista, M. *Spectrochim. Acta, Part A* **1995**, *51*, L7−L21.
(32) McHedlovpetrosyan, N. O.; Vasetskaya, L. V. *Zh. Obshch. Khim.* **1989**, *59*, 691−703.
(33) McHedlov-Petrossyan, N. O.; Tychina, O. N.; Berezhnaya, T. A.; Alekseeva, V. I.; Savvina, L. P. *Dyes Pigm.* **1999**, *43*, 33−46.
(34) Fompeydie, D.; Onur, F.; Levillain, P. *Bulletin De La Societe Chimique De France Partie I-Physicochimie Des Systemes Liquides Electrochimie Catalyse Genie Chimique* **1979**, 375−380.
(35) Seybold, P. G.; Gouterman, M.; Callis, J. *Photochem. Photobiol.* **1969**, *9*, 229−42.
(36) McCreery, R. L. *Meas. Sci. Technol* **2001**, *12*, 653.